Mem. S.A.It. Vol. 76, 150

Memorie della

Infrared emission from the dusty veil around AGN

Thomas Beckert

Max-Planck-Institut für Radioastronomie, Auf dem Hügel 69, 53121 Bonn, Germany e-mail: tbeckert@mpifr-bonn.mpg.de

Abstract. We discuss consequences of the concept of a clumpy and dusty torus around AGN. Cloud-cloud collisions lead to an effective viscosity and a geometrically thick accretion disk, which has the required properties of a torus. A quantitative comparison of radiative transfer calculations for dust re-emission from the torus with NIR images, long-baseline visibilities and spectral energy distributions for the torus in the Seyfert nucleus of NGC 1068 is presented.

Key words. AGN – torus – infrared – NGC 1068

1. Introduction: Dusty tori in the unified model of AGN

The unified model of AGN, which emerged from the interpretation spectropolarimetry of NGC 1068 (Miller & Antonucci 1983), explains the difference between type 1 and type 2 AGN with aspect-angle-dependent obscuration by a dusty torus or thick disk. In the simplest unification scheme all Seyfert 2 nuclei harbor a Seyfert 1 core, so that the ratio of type 1s to 2s, which varies between 1:4 (Maiolino & Rieke 1995) and to 1:1 (Lacy t al. 2004) measures the thickness of the torus. The torus should therefore have a half opening ratio $H/R \sim 1$.

Krolik & Begelman (1988) argued that these tori must consist of a large number of individual dusty clouds. The clumpiness was not included in the following radiative transfer calculations (e.g., Pier & Krolik 1992; Granato & Danese 1994) of dust re-emission from these tori. Nenkova et al. (2002) realized that the clumpiness might be important for the appearance of the tori and developed an approximative and statistical scheme which accounts for the clumpiness in radiative transfer calculations of the thermal infrared emission from clouds, which are individually optically thick $\tau_V > 40$. This approach resolved some of the problems with earlier radiative transfer calculations. In this paper we summarize the model of a dynamical equilibrium of quasi-stable dusty clouds in the gravitational potential of an galactic nucleus described in Vollmer et al. (2004) and Beckert & Duschl (2004).

2. Cloud distribution and their properties in the torus

The equilibrium model of cold, dusty clouds is distinctively different from the multi-phase medium in the general ISM of a galaxy (Vollmer et al. 2004), in so far, as the clouds are quasi-stable and experience frequent cloud-cloud collisions. These collisions are the domi-

Send offprint requests to: T. Beckert
Correspondence to: Auf dem Hügel 69, 53121 Bonn, Germany

nant process for the creation and destruction of clouds. The mass and size of the largest clouds in the torus is limited by the shear in the gravitational potential of the galactic nucleus and the internal pressure support against their own gravity. Their size and mass is given by the shear limit and the Jeans limit for a given internal sound speed c_s. In a model for the distribution of clouds (Beckert & Duschl 2004) we decouple the the vertical and radial structure as is usually done for geometrically thin accretion disks, despite the thickness of the torus.

The important parameter of the torus in radiative transfer calculations is the vertical optical depth for intercepting a cloud

$$\tau = \int \mathrm{d}z \, l_{\mathrm{coll}}^{-1} , \tag{1}$$

where l_{coll} is the mean free path of clouds in the torus. We expect that clouds accumulate at the shear limit when they experience increasing tidal forces while being accreted to the center. The upper limit to the cloud size corresponds to a lower limit of the torus surface density

$$\Sigma \geq \frac{\tau}{\sqrt{8}} \frac{M(R)}{R^2} \frac{c_s}{v_\phi} . \tag{2}$$

Here $M(R)$ is the total enclosed mass at radius R and v_ϕ is the Keplerian circular velocity at that radius.

For the distribution of clouds in the torus we assume hydrostatic equilibrium for the vertical stratification. In Beckert & Duschl (2004) we used a modified isothermal distribution function of cloud velocities in an external potential, which includes a cut-off scale height x_H at which the density drops to zero. This leaves room for a wide polar outflow cavity. The cut-off height is larger than the pressure scale height H in all models. An example for the case of NGC 1068 is shown in Fig. 1. The radial structure is derived from a stationary accretion scenario.

3. Cloud collisions and accretion

The optical depth τ defined in Eq. (1) has to be $\tau \sim 1$ for obscuration of the AGN for line of sights through the torus. Because τ is

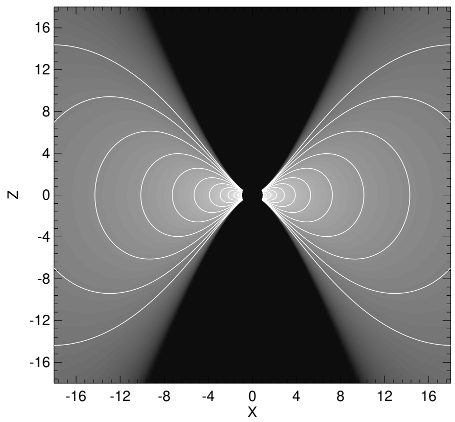

Fig. 1. Meridional cut through the probability density distribution of finding a dusty cloud in the torus. The distribution leaves room for an outflow along the polar axis. The spatial scale is in units of the dust sublimation radius. The mean number of clouds along a line of sight to the center drops below 1 for angels larger that 40° from the midplane ($Z = 0$).

also a dimensionless collision frequency $\tau \sim \omega_c/\Omega$, this implies that cloud-cloud collisions are frequent in a torus. For anisotropic velocity dispersions of clouds Goldreich & Tremaine (1978) derived a sufficient approximation for the effective viscosity

$$\nu = \frac{\tau}{1+\tau^2} \frac{\sigma^2}{\Omega} \tag{3}$$

for angular momentum redistribution. The required anisotropy can be determined self-consistently for thin accretion disks and we use this limit also for the torus.

Like in ordinary accretion disks, the effective viscosity from Eq. (3) allows mass to be accreted towards the black hole. For the special case of a dusty torus attention must be paid to the proper inner boundary condition for the conservation law of angular momentum of the cloud distribution. The inner boundary will be at the sublimation radius for dust ($R \sim 1$ pc), where neither torque nor shear will vanish. In addition the torque at the inner boundary is most likely not well described by the viscosity (Eq. 3).

In cloud-cloud collisions a fraction $\frac{1}{2}(1-\epsilon^2)$ of the average relative kinetic energy of clouds is dissipated, where ϵ is the coefficient of restitution, which approaches 1 for elastic collisions. In a stationary model ϵ ties the release of gravitational binding energy due to accretion to the dissipation in cloud collisions. Contrary to thin disks values of ϵ in the range $0.2-0.6$ are possible in geometrically thick tori, because of energy advection.

4. The Torus in NGC 1068

For a comparison of spectral energy distribution (SED) and surface brightness distribution or morphology of a particular AGN the mass distribution has to be known or modeled. For the case of NGC 1068 we collected the available data in Beckert & Duschl (2004). An important caveat must be pointed out: The rotation of the ring of H_2O-maser spots (Greenhill & Gwinn 1997) tends to underestimate the enclosed mass and this may be the reason why the derived rotation appears not to be due to a central point mass (black hole). Only in a very thin disk like in NGC 4258 the projected radial velocities will follow a Keplerian profile. The thickness of the the free-free disk (component S1 of the radio jet) in NGC 1068 (Gallimore et al. 2004) and the intermediate orientation of the maser disk might imply a larger velocity dispersion of maser spots. Their projected radial velocities will then span a wider range of sub-Keplerian velocities. So it may well be that the mass of the central black hole is larger than $10^7\,M_\odot$.

We have used the model for individual clouds in a torus, and the cloud density distribution shown in Fig. 1 for a mass accretion rate of $6\,M_\odot$/yr through the torus and a coefficient of restitution $\epsilon = 0.4$ in cloud collisions to derive a surface brightness distribution (Fig. 2) and SED (Fig. 3) based on radiative transfer calculations with the method of Nenkova et al. (2002). We find a size of 0.9 pc for the dust sublimation radius consistent with the size of the observed core component in speckle images (Weigelt et al. 2004) in the NIR. The implied AGN luminosity is $L = 2.4\,10^{45}$ erg/s and therefore larger than the Eddington limit for a $10^7\,M_\odot$ black hole.

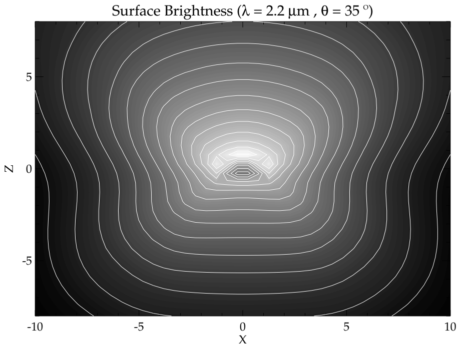

Fig. 2. K-band brightness distribution of our radiative transfer calculations based on the method of Nenkova et al. (2002) and the scenario of Beckert & Duschl (2004) for an inclination of 35° from the midplane. The spatial scale is in units of the dust sublimation radius. The contour scale of the surface brightness is logarithmic with a dynamic range of 2^{14}.

5. Implications

While the overall shape of the SED and the size of the sublimation radius conform with observations, the shape of the silicate absorption feature (Fig. 3) measured with MIDI (Jaffe et al. 2004) does not. We have not yet systematically searched the parameter space for the torus to exclude the normal interstellar dust mixture used in our simulations. But we tentatively agree with Jaffe et al. (2004) that the grain size distribution and/or the dust chemical composition is different close to the AGN in NGC 1068.

The clumpiness of the torus can explain the seemingly disparate results of K'-band speckle images and the K-band long-baseline visibility ($b = 46$ m) of Wittkowski et al. (2004). The interferometry result can either set an upper limit to the size of individual clouds $R_{\rm Cl} < 0.4$ pc and super-resolves the separation between clouds, or it indicates a low-extinction view of the central accretion flow, which has a non-negligible probability for a clumpy torus. In addition, the surprisingly large K'-band flux

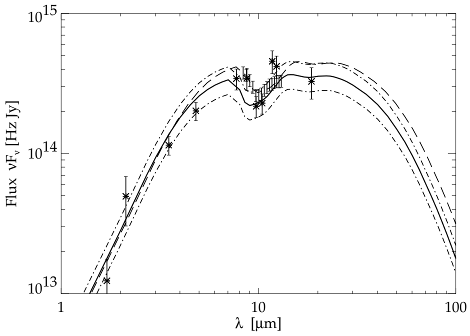

Fig. 3. Spectrum of a clumpy torus model with normal interstellar dust composition adapted for NGC 1068. The assumed inclination from the torus midplane is $i = 35°$ and the coefficient of restitution is $\epsilon = 0.4$. The required mass accretion rate through the torus is $6\,M_\odot\,\mathrm{yr}^{-1}$ is this model. The required AGN luminosity is $L_{45} = 2.4 \pm 0.3$ in units of 10^{45} erg s^{-1}, which corresponds to about twice the Eddington luminosity of a $9\,10^6\,M_\odot$ black hole. The solid line corresponds to the mean luminosity and the dash-dotted lines indicted the range of uncertainty. The silicate absorption feature as measured with MIDI (Jaffe et al. 2004) is not well fitted. An unacceptable modification, which does fit the data (dashed line), is achieved by an artificial redshift of $\Delta\lambda/\lambda = 0.1$ and a luminosity of $L_{45} = 2.7$.

of 350 mJy of Weigelt et al. (2004) might be due to an additional contribution from optically thin synchrotron emission (Beckert & Duschl 1997) as already suggested by Wittkowski et al. (1998). The large mass accretion rate through the the torus, which is required to keep the torus geometrically thick and the number of clouds along a line of sight through the torus low ($\leq$ 10), implies that only a small fraction of the mass accreted through the torus eventually reaches the black hole.

References

Beckert, T. & W. J. Duschl, W. J. 1997, A&A 328, 95

Beckert, T. & W. J. Duschl, W. J. 2004, A&A 426, 445

Gallimore, J. F., Baum, S. A., O'Dea, C. P. 2004, ApJ, 613, 794

Goldreich, P. & Tremaine S. 1978, Icarus, 34, 227

Granato, G. L. & Danese, L. 1994, MNRAS, 268, 235

Greenhill, L. J. & Gwinn, C. R. 1997, Ap&SS, 248, 261

Jaffe, W., Meisenheimer, K., Röttgering, H. J. A., et al. 2004, Nature 429, 47

Krolik, J. H. & Begelman, M. C. 1988, ApJ 329, 702

Lacy, M., Storrie-Lombardi, L. J., Sajina, A. et al. 2004 ApJS, 154, 166

Maiolino, R. & Rieke, G. H. 1995, ApJ, 454, 95

Miller, J. S. & Antonucci, R. R. J. 1983, ApJ, 271, L7

Nenkova, M., Ivezić, Ž., Elitzur, M. 2002, ApJ 570, L9

Pier, E. A. & Krolik, J. H. 1992, ApJ, 401, 99

Vollmer, B., Beckert, T., Duschl, W. J. 2004, A&A, 413, 949

Weigelt, G., Wittkowski, M., Balega, Y. Y., Beckert T., et al. 2004, A&A, 425, 77

Wittkowski, M., Balega, Y., Beckert, T., Duschl, W. J., Hofmann, K.-H, Weigelt, G. 1998, A&A 329, L45

Wittkowski, M., Kervella, P., Arsenault, R., Paresce, F., Beckert, T., Weigelt, G. 2004, A&A 418, L39